DOI: 10.1002/cbic.201100716

Versatile Effects of Aurone Structure on Mushroom Tyrosinase Activity

Carole Dubois,[a] Romain Haudecoeur,[b] Maylis Orio,[c] Catherine Belle,[c] Constance Bochot,[c] Ahcène Boumendjel,[b] Renaud Hardré,[a] Hélène Jamet,[c] and Marius Réglier*[a]

Dedicated to Andreas Heumann on the occasion of his 70th birthday

Elucidation of the binding modes of Ty inhibitors is an important step for in-depth studies on how to regulate tyrosinase activity. In this paper we highlight the extraordinarily versatile effects of the aurone structure on mushroom Ty activity. Depending on the position of the OH group on the B-ring, aurones can behave either as substrates or as hyperbolic activators. The synthesis of a hybrid aurone through combination of an aurone moiety with HOPNO (2-hydroxypyridine *N*-oxide), a good metal chelate, led us to a new, efficient, mixed inhibitor for mushroom tyrosinase. Another important feature pointed out by our study is the presence of more than one site for aurone compounds on mushroom tyrosinase. Because study of the binding of the hybrid aurone was difficult to perform with the enzyme, we undertook binding studies with tyrosinase functional models in order to elucidate the binding mode (chelating vs. bridging) on a dicopper(II) center. Use of EPR combined with theoretical DFT calculations allowed us to propose a preferred chelating mode for the interaction of the hybrid aurone with a dicopper(II) center.

Introduction

Tyrosinases (Ty's, EC 1.14.18.1) are ubiquitous copper-containing enzymes belonging to the type-3 or "coupled binuclear" family.[1,2] Ty's catalyze the two-step oxidation of phenolic compounds into the corresponding catechols (monophenolase activity) and *ortho*-quinones (catecholase activity). In mammals, their biological function is to convert L-tyrosine into dopaquinone, which is the key product for melanin pigment biosynthesis. Melanin-related disorders are known to cause serious skin lesions,[3] Parkinson's disease,[4] and melanoma.[5] In addition, Ty's are responsible for the browning of plant foods, which creates an important economic problem in the field of nutrition. Ty inhibition is a well-established approach for controlling in vivo melanin production and food browning, so the development of Ty inhibitors has a huge economical and industrial impact, as is illustrated by the increasing number of Ty inhibitors described in the recent literature.[6] A large proportion of this literature is devoted to naturally occurring compounds. Among these, aurones are particularly attractive because they have been reported as inhibitors of melanin synthesis in human melanocytes.[7] Some of these naturally occurring Ty inhibitors target the Ty binuclear copper active site. These inhibitors are named transition state (TS) analogues; they have structural analogies to catechol but are not oxidizable. Thujaplicin,[8] kojic acid,[9] and L-mimosin[10] are good illustrations of this strategy. Recently, we reported on 2-hydroxypyridine-*N*-oxide (HOPNO) as a non-naturally occurring TS analogue Ty inhibitor with a competitive inhibition constant of 1.8 μM.[11] Because HOPNO is well known as good metal chelate,[12] we might suspect some lack of specificity, which could limit its use. In order to improve the specificities of HOPNO moieties towards Ty, we investigated the synthesis and evaluation of a HOPNO compound embedded in an aurone backbone. In this paper we report on the evaluation of aurone derivatives **1a–e** on mushroom Ty activity and on the synthesis of the hybrid aurone **2** and its evaluation as an inhibitor of mushroom Ty.

Results and Discussion

Versatile effects of aurones on mushroom Ty activity

In a previous study, the most potent aurones were found to be those bearing a hydroxy group at the 4′-position of the B-ring.[7] In the belief that aurones interact with the binuclear copper active site through this ring, we made a study of aurones in which the position of the hydroxy group on the A-

[a] *C. Dubois,[+] Dr. R. Hardré, Dr. M. Réglier*
Institut des Sciences Moléculaires de Marseille, Équipe BiosCiences
UMR-CNRS 7313, Aix–Marseille Université
avenue Escadrille Normandie-Niemen
13397 Marseille Cedex 20 (France)
E-mail: marius.reglier@univ-amu.fr

[b] *R. Haudecoeur,[+] Prof. A. Boumendjel*
Département de Pharmacochimie Moléculaire, Université Joseph Fourier
UMR-CNRS 5063, ICMG FR-2607
B.P. 53, 38041 Grenoble Cedex 9 (France)

[c] *Dr. M. Orio,[+] Dr. C. Belle, Dr. C. Bochot, Dr. H. Jamet*
Département de Chimie Moléculaire, Équipes Chimie Théorique et CIRE
Université Joseph Fourier
UMR-CNRS 5250, ICMG FR-2607
B.P. 53, 38041, Grenoble Cedex 9 (France)

[+] *These authors contributed equally to this work.*

Supporting information for this article is available on the WWW under http://dx.doi.org/10.1002/cbic.201100716.

ring is fixed in the 6-position and the one on the B-ring varies (compounds **1a**–**e**). The effect of compounds **1a**–**e** on Ty-catalyzed L-DOPA oxidation revealed the versatile effects of the aurone structure.

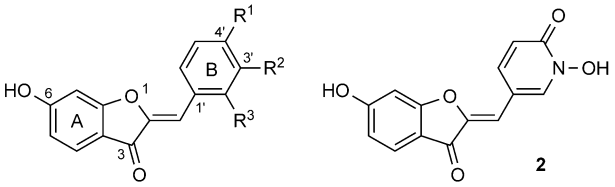

1a: ($R^1 = R^2 = R^3 = H$)
1b: ($R^1 = OH; R^2 = R^3 = H$)
1c: ($R^1 = H; R^2 = OH; R^3 = H$)
1d: ($R^1 = R^2 = H; R^3 = OH$)
1e: ($R^1 = R^2 = OH; R^3 = H$)

In this study, we used a commercially available mushroom Ty that we purified on a Q-sepharose FF chromatographic column by a known procedure.[13] For Ty-catalyzed L-DOPA oxidation, we determined the Michaelis–Menten kinetic parameters—$K_m = 0.31 \pm 0.6$ mM and $V = 0.87 \pm 0.06$ μM s^{-1}—by measuring the increase in absorbance at 475 nm, which corresponds to the formation of the DOPAchrome (Figure S1 in the Supporting Information).

Whereas aurone **1a** exhibits no activity, the others behave either as substrates (**1b** and **1e**) or as hyperbolic activators (**1c** and **1d**), depending on the position(s) of the hydroxy group(s) on the B-ring. The UV–visible spectra of aurones **1a**–**e** were checked in the presence of mushroom Ty. This experiment revealed that the *para*-phenol **1b** undergoes a transformation as a result of Ty-catalyzed oxidation. In the UV–visible spectrum (300–600 nm, Figure 1) of aurone **1b** in phosphate buffer (pH 7, 50 mM) containing Ty (3.3 μg), the decrease in the intensity of the band at 400 nm and concomitant increase in the one at 499 nm, together with the two isosbestic points at 348 and 446 nm, indicate a transformation into an unique compound that should be a quinone resulting from oxidation of phenol either on the A- or on the B-ring.

Under the same conditions, the catechol aurone **1e** also undergoes a transformation as revealed by a decrease in the intensity of the band at 414 nm with an isosbestic point at 367 nm (Figure S2).

Because of their instability, all of our attempts to characterize products formed during the Ty-catalyzed oxidation of aurones **1b** and **1e** failed. We overcame this problem by addition of $NaBH_3CN$ at the end of the reaction in order to reduce the formed quinone into a more stable catechol (Scheme 1). HPLC analysis (C18, 3% AcOH in water/acetonitrile) of the reduced mixtures revealed the formation of aurone **1e** (30%) during Ty-catalyzed oxidation of **1b**, as confirmed with an authentic sample of **1e** (Figure S3).

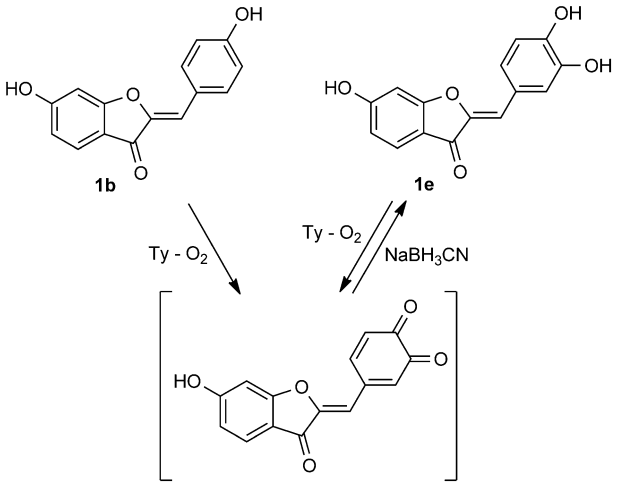

Scheme 1. Ty-catalyzed oxidations of the *para*-phenol **1b** and the catechol **1e** and quinone trapping by $NaBH_3CN$.

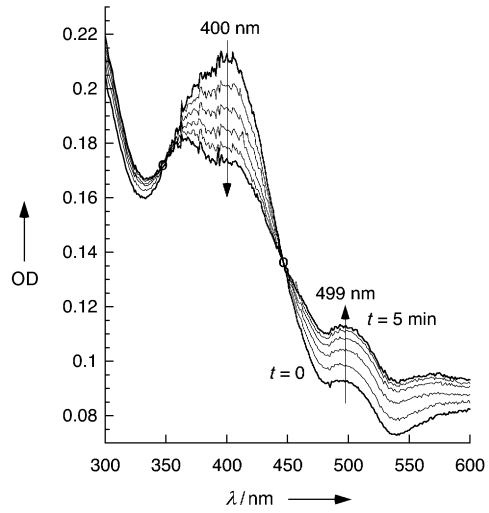

Figure 1. Absorption spectra of **1b** (4.37 μM) in phosphate buffer (50 mM, pH 7) in the presence of mushroom Ty (3.3 μg). Spectra were scanned every minute until 5 min.

For the two substrates **1b** and **1e**, we determined the kinetic features of the Ty-catalyzed oxidation by measuring the decreases in the absorption bands at 400 nm. The kinetics of Ty-catalyzed oxidation of aurones **1b** and **1e** exhibit non-Michaelis–Menten behavior with sigmoid shapes according to a cooperative mechanism (Figure 2). A classical treatment according to the Hill equations[14] [Eqs. (1), (2), and (3)] leads to the macroscopic kinetic features V, $K_{0.5}$, and h (Hill coefficients) for these two substrates [**1b**, $V = (0.40 \times 10^{-3} \pm 0.02 \times 10^{-3})$ $\Delta OD\, s^{-1}$, $K_{0.5} = 365 \pm 32$ μM, and $h = 2.05 \pm 0.22$; **1e**, $V = (2.21 \times 10^{-3} \pm 0.05 \times 10^{-3})$ $\Delta OD\, s^{-1}$ and $K_{0.5} = 28 \pm 2$ μM and $h = 1.87 \pm 0.17$].

$$V = \frac{V \times S^h}{K_{0.5}^h + S^h} \quad (1)$$

$$\frac{V}{V - v} = \frac{S^h}{K_{0.5}^h} \quad (2)$$

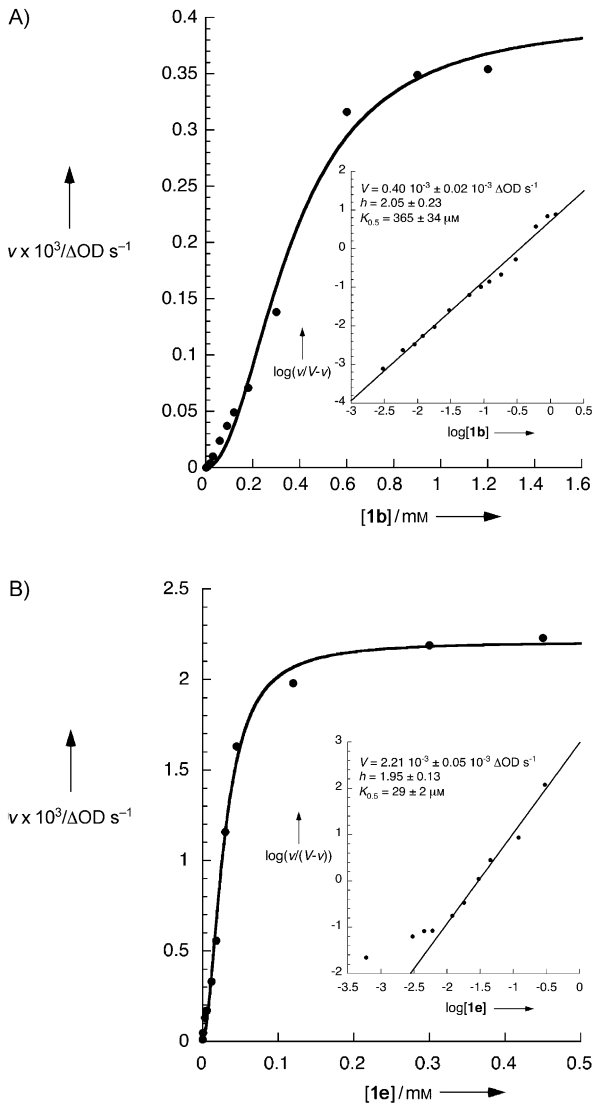

Figure 2. Plots of initial rates of Ty-catalyzed oxidation of A) **1 b**, and B) **1 e** vs. substrate concentrations (fitting according to the Hill equation, goodness of fit $R = 0.99641$ and 0.99711, respectively); Hill plots in insets. Conditions: phosphate buffer (50 mM, pH 7) in the presence of mushroom Ty (6.4 μg mL^{-1}).

$$\log\left[\frac{V}{V-v}\right] = h\,(\log S - \log K_{0.5}) \qquad (3)$$

Although the UV–visible spectra of *meta*-phenol **1 c** and *ortho*-phenol **1 d** were not modified by Ty-catalyzed oxidation (Figure S4), they behave as activators in the presence of the substrate L-DOPA. Indeed, they exhibit dose-dependent activation in Ty-catalyzed oxidation of L-DOPA (**1 c**, 214% and **1 d**, 118% activation at 300 μM for [L-DOPA] = 2.8 mM; Figure 3 B). Classical treatment involving plotting of $1/V^{app}$ against reciprocal activator concentration showed that the aurones **1 c** and **1 d** behave as hyperbolic activators (Figure 3 A).[14]

The cooperativity in Ty-catalyzed oxidations of aurones **1 b** and **1 e** suggests that they interact with mushroom Ty at at least two different sites: a catalytic site and one allosteric site that increases the enzyme activity. The Hill coefficients, measures of cooperativity in binding processes, indicate that the binding of one ligand facilitates the binding of a subsequent ligand at the catalytic site. This proposal is supported by the Ty activation by aurones that are not substrates—the *meta*-phenol **1 c** and *ortho*-phenol **1 d**. These molecules interact with Ty at at least one site, which increases the Ty activity. Activation of latent Ty from plant and insect sources is well known, but is rare for mushroom Ty.[6] Activation of mushroom Ty by SDS,[15] benzyl alcohol,[16] 3-hydroxyanthranilic acid,[17] and 3-hydroxykynurenine[18] has been reported. This activation is often attributed to conformational changes on Ty or to removal of an inhibitor during the purification. The proposal that aurone compounds could interact with mushroom Ty at at least two sites is particularly important because the recently published structure confirms that mushroom Ty exists as a H_2L_2 tetramer.[19] However, we cannot definitively exclude the possibility that these effects could be due to the presence of Ty isoforms with different kinetic features.

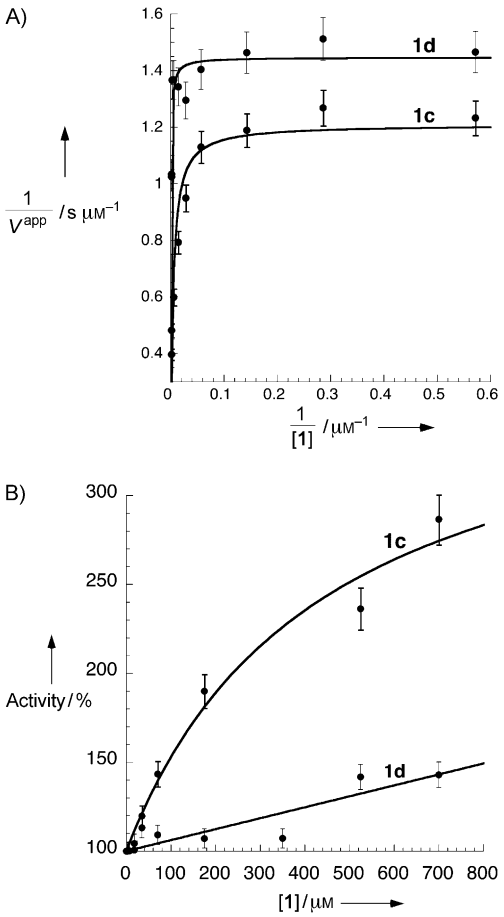

Figure 3. Hyperbolic activation of mushroom Ty by aurones **1 c** and **1 d**. Conditions: phosphate buffer (50 mM, pH 7), [L-DOPA] = 2.8 mM, [Ty] = 6.4 μg mL^{-1}.

HOPNO embedded on aurone—synthesis and mushroom Ty inhibition

With the goal of finding new Ty inhibitors, we combined aurone recognition by mushroom Ty with the inhibition potential of HOPNO. Because we have shown that the aurones interact with the dinuclear copper active site through their B-rings, we prepared the new aurone **2** in which the B-ring is replaced by a HOPNO moiety. The synthesis of aurone **2** (Scheme 2) was

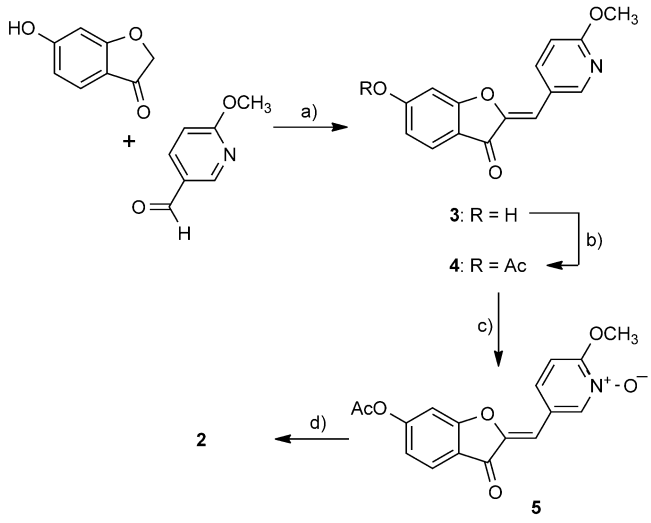

Scheme 2. Synthesis of aurone **2**: a) KOH, CH_3OH, 65 °C, 2 h, 93%; b) Ac_2O, 140 °C, 5 h, 96%; c) H_2O_2/urea, TFAA, CH_2Cl_2, RT, 16 h, 63%; d) HCl, CH_3OH, 100 °C, 16 h, 83%.

performed by starting from 6-hydroxybenzofuran-3(2*H*)-one, prepared by the known reported method.[20] It was condensed with 6-methoxypyridine-3-carbaldehyde, followed by protection of the phenol groups. N-Oxidation with H_2O_2/urea adduct and deprotection under acidic conditions afforded the aurone **2**, which was obtained with a good overall yield and a high analytical purity.

The effect of aurone **2** on the oxidation of L-DOPA by mushroom Ty was studied. We first determined that the Ty inhibition was concentration-dependent, with an IC_{50} estimated as 1.5 ± 0.2 μM (Figure S5). The kinetic behavior of mushroom Ty during the oxidation of L-DOPA was then investigated. Aurone **2** exhibits mixed inhibition features, as revealed by a graphical method consisting of plotting $1/v$ (Dixon plot) and [L-DOPA]/v against the inhibitor concentration (Figure S6). The macroscopic kinetic features for the competitive inhibition (K_{ic}) and the uncompetitive inhibition (K_{iu}) were determined by evaluation of V^{app} and K_m^{app} from the Michaelis–Menten plot at different concentrations of **2** (Figure 4a).[14] From Equation (4) and the $1/V^{app}$ versus [**2**] plot, we extracted $K_{iu} = 1.62 \pm 0.28$ μM, whereas from Equation (5) and the K_m^{app}/V^{app} vs. [**2**] plot it was determined that $K_{ic} = 1.27 \pm 0.16$ μM.

$$\frac{1}{V^{app}} = \frac{1}{V} \times \left(1 + \frac{I}{K_{iu}}\right) \quad (4)$$

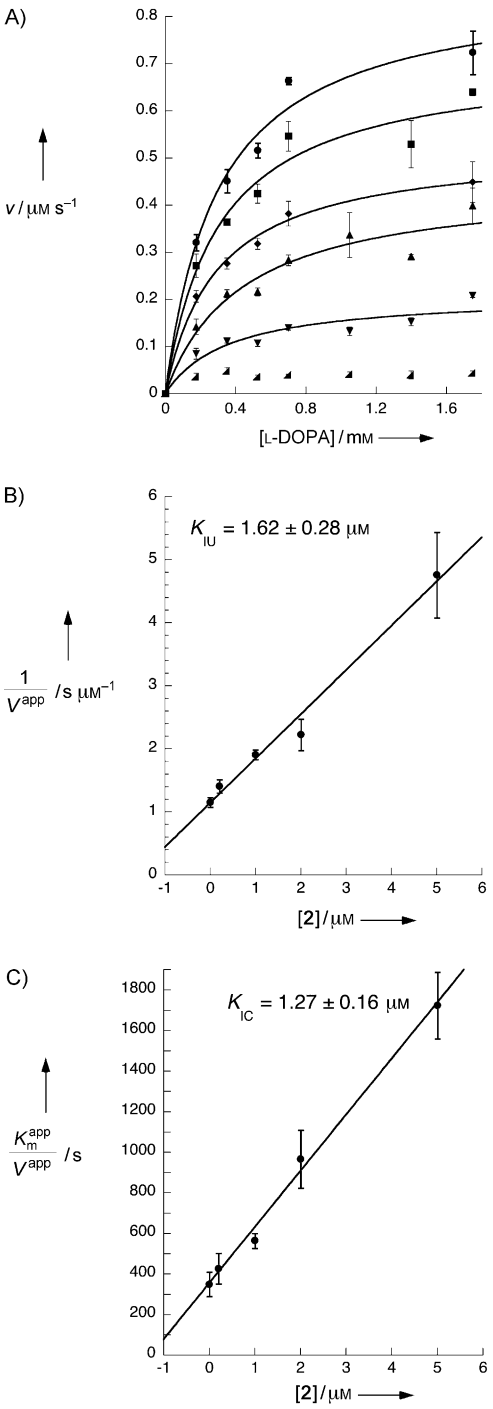

Figure 4. Inhibition of mushroom Ty by aurone **2**. Conditions: phosphate buffer (50 mM, pH 7), [Ty] = 6.4 μg mL^{-1}. Dependence: A) of the initial rate (v_i) on [L-DOPA] at various [**2**] (● = 0, ■ = 0.2, ◆ = 1, ▲ = 2, ▼ = 5, ◢ = 20 μM), B) of $1/V^{app}$ on [**2**], and C) of K_m^{app}/V^{app} on [**2**].

$$\frac{K_m^{app}}{V^{app}} = \frac{K_m}{V} \times \left(1 + \frac{I}{K_{ic}}\right) \quad (5)$$

Aurone **2** has an activity similar to that of HOPNO ($K_{ic} = 1.8$ μM),[11] but with different features (competitive vs. mixed inhibition). However, with aurone **2** we can expect an increase in the selectivity with respect to Ty. The mixed inhibition features

of **2** again suggest a multiple binding site for this derivative. The deciphering of its binding mode is an important step for studies on how to regulate the Ty activity.

Binding studies

The evaluation of the inhibition properties of **2** gives evidence that this compound interacts in part with the Cu ions in the binuclear active site of the enzyme. We set out to study the interaction of **2** with mushroom Ty by UV–visible spectroscopy. Unfortunately, the addition of **2** to mushroom Ty produced no observable change in the UV–visible spectrum, and so we oriented our study on the interaction of **2** on Ty complex models. A first approach to obtain more insight into its binding mode at the Ty active site was to study inhibitor interactions with a low-molecular-weight binuclear copper system mimicking the dicopper(II) center of the enzyme, combining experimental and theoretical investigations. In this way, through the use of the binuclear copper(II) complex $[Cu_2(BPMP)(\mu\text{-}OH)](ClO_4)_2$ [**I**·$(ClO_4)_2$], known as a functional model for the Ty catecholase activity,[21] we have previously shown that deprotonated HOPNO chelates only one Cu atom of the binuclear site in a chelating mode (Scheme 3).[11]

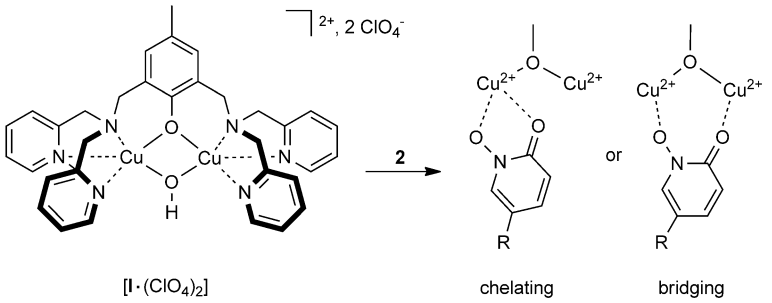

Scheme 3. $[Cu_2(BPMP)(\mu\text{-}OH)](ClO_4)_2$ as a functional model for Ty catecholase activity and possible binding modes for **2** at the dicopper(II) center.

Unfortunately, attempts to isolated some adducts with **2** in the solid state have so far been unsuccessful. Nevertheless, the X-band EPR spectrum of [**I**·$(ClO_4)_2$] after the addition of 1 equiv of **2** in frozen solution [HEPES (pH 7)/DMSO 1:1] suggests a change in copper coordination geometry and supports the binding of **2** at the dicopper center (Figure S7). The spectrum reveals a weak $\Delta Ms \pm 2$ transition around 150 mT and a broad $\Delta Ms \pm 1$ signal from 230 to 400 mT, which is characteristic of slightly magnetically coupled copper(II) ions, whereas [**I**·$(ClO_4)_2$] is EPR-silent, in accordance with the relatively strong antiferromagnetic coupling between the copper ions [$J = (-112 \pm 2)$ cm^{-1}, with $H = -2\,JS_1 \cdot S_2$; $S_1 = S_2 = {}^1/_2$).[21]

In order to get some information on the $\mathbf{I}^{2+} + \mathbf{2}$ binding mode, theoretical calculations were undertaken. The two different binding modes shown in Scheme 3 were considered and possible $\mathbf{I}^{2+} + \mathbf{2}$ adducts formed are shown in Figure 5. They are designated **2**-bg and **2**-ch, for the bridging and the chelating modes, respectively. Because no X-ray experimental data

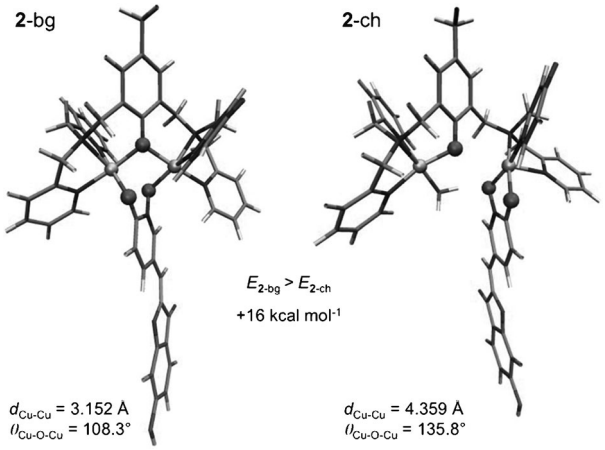

Figure 5. Graphical representation of the binding modes (**2**-bg: bridging, **2**-ch: chelating) for adducts of complex $\mathbf{I}^{2+}$ with **2**.

are available for $\mathbf{I}^{2+} + \mathbf{2}$, the DFT-predicted structures of the two binding modes are compared exclusively on the basis of the computational results. The chelating mode shows an elongated Cu–Cu interatomic distance relative to the bridging mode. Consequently, the exchange interaction between the two copper centers becomes less efficient and a weak ferromagnetic coupling ($J = 12$ cm^{-1}) is calculated for this mode. On the other hand, the two Cu centers in **2**-bg are antiferromagnetically coupled ($J = -255$ cm^{-1}). These data, in conjunction with the EPR spectrum mentioned before, suggest that **2** is linked to $\mathbf{I}^{2+}$ in a chelating mode. To confirm this result, we compared the relative stabilities of the two modes with the aid of a computational approach described in the Supporting Information. Results of the energetic analysis are shown in Figure 5. Our calculations predict that **2**-ch should be the more favored binding mode, with an energetic stabilization of 16.0 kcal mol^{-1}. This is the same binding mode that we found for HOPNO on $\mathbf{I}^{2+}$.[11]

Conclusions

Deciphering the binding modes of Ty inhibitors is an important step for in-depth studies on how to regulate the tyrosinase activity. Our results highlight the extraordinarily versatile effects of the aurone structure on mushroom Ty activity. Depending on the position of the hydroxy group on the B-ring, aurones can behave as substrates (**1b** and **1e**), as hyperbolic activators (**1c** and **1d**), or—in the particular case of the hybrid aurone **2**—as a mixed inhibitor. This last compound has been identified as a new and efficient inhibitor for mushroom Ty. Another important feature highlighted in our study is the presence of multiple binding sites for aurone compounds on mushroom

Ty. In addition to the active site where substrates bind, at least one other site could be responsible for activation due to modification of interactions between the H and L subunits of mushroom Ty.

Because the study of the binding of **2** was difficult to carry out on mushroom Ty, we undertook binding studies with Ty functional models in order to elucidate the binding mode (chelating or bridging) on a dicopper(II) center. With the aid of a combined EPR study with theoretical DFT calculations, we proposed a preferred chelating mode (**2**-ch) for the interaction of aurone **2** with a dicopper(II) center. These results are of primary importance because with this set of structural data (**2**-bg vs. **2**-ch) we can envisage an EXAFS/XANES study in order to decipher the binding mode of aurones and then propose new scaffolds that might better target the Ty metal active site for more selective and potent inhibitor development.

Experimental Section

Syntheses: ^{1}H and ^{13}C NMR spectra were recorded with a Brüker Advance 400 instrument (400 MHz for ^{1}H, 100 MHz for ^{13}C). Chemical shifts are reported relative to Me_4Si as internal standard. ESI mass spectra and elemental analyses were performed at the analysis facilities of the department of chemistry of the University of Grenoble, France. Thin-layer chromatography (TLC) was carried out with Merck silica gel F-254 plates (0.25 mm thick). Flash chromatography was carried out with Merck silica gel 60, 200–400 mesh. All solvents were distilled prior to use. Chemicals and reagents were obtained either from Aldrich or Acros and were used as obtained.

(*Z*)-6-Hydroxy-2-((6-methoxypyridin-3-yl)methylene)benzofuran-3(2*H*)-one (3): An aqueous solution of potassium hydroxide (50%, 7 mL) was added to a solution of 6-hydroxybenzofuran-3(2*H*)-one (963 mg, 6.42 mmol) in methanol (100 mL), followed by the addition of 6-methoxypyridine-3-carbaldehyde (880 mg, 6.42 mmol). The mixture was heated at reflux for 2 h, and the methanol was then evaporated. The residue was diluted in water and a solution of aqueous hydrochloric acid (10%) was added to adjust the pH to 2–3. The resulting precipitate was filtered and washed successively with water, acetonitrile, and diethyl ether to afford hydrochloride salt of the title compound (1.82 g, 93%) as a pale yellow solid: m.p. 260–262 °C (decomp.); ^{1}H NMR (400 MHz, [D$_6$]DMSO): $\delta =$ 11.25 (s, 1H; OH), 8.66 (s, 1H; 2′-H), 8.28 (d, $J = 8.0$ Hz, 1H; 6′-H), 7.60 (d, $J = 8.0$ Hz, 1H; 4-H), 6.93 (d, $J = 8.0$ Hz, 1H; 5′-H), 6.79 (s, 1H; –CH=), 6.79 (s, 1H; 7-H), 6.71 (d, $J = 8.0$ Hz, 1H; 5-H), 3.89 ppm (s, 3H; OMe); ^{13}C NMR (100 MHz, [D$_6$]DMSO): $\delta = 181.1$ (C-3), 167.8 (C-6), 166.6 (C-8), 163.8 (C-4′), 150.4 (C-2′), 147.2 (C-2), 140.4 (C-6′), 126.0 (C-4), 122.1 (C-1′), 113.1 (C-9), 112.9 (C-7), 111.2 (–CH=), 107.4 (C-5′), 98.7 (C-5), 53.6 ppm (OMe); MS (ESI): *m/z*: 270 $[M+H]^+$; elemental analysis calcd (%) for $C_{15}H_{11}NO_4 \cdot {}^3/_4$ HCl: C 60.73, H 3.96, N 4.72; found: C 60.54, H 4.30, N 4.80.

(*Z*)-6-Acetoxy-2-((6-methoxypyridin-3-yl)methylene)benzofuran-3(2*H*)-one (4): A solution of (*Z*)-6-hydroxy-2-((6-methoxypyridin-3-yl)methylene)benzofuran-3(2*H*)-one (**3**, 378 mg, 1.41 mmol) in acetic anhydride (8 mL) was heated at reflux for 5 h. After cooling, the mixture was poured into water (60 mL) and was then extracted with dichloromethane, washed with water and brine, dried over magnesium sulfate, and concentrated under reduced pressure to afford the title compound (419 mg, 96%) as a pale yellow solid: m.p. 190–192 °C; ^{1}H NMR (400 MHz, $CDCl_3$): $\delta = 8.60$ (d, $J = 2.4$ Hz, 1H; 2′-H), 8.23 (dd, $J_1 = 8.7$ Hz, $J_2 = 2.4$ Hz, 1H; 6′-H), 7.82 (d, $J =$ 8.3 Hz, 1H; 4-H), 7.14 (d, $J = 1.8$ Hz, 1H; 7-H), 6.97 (dd, $J_1 = 8.3$ Hz, $J_2 = 1.8$ Hz, 1H; 5-H), 6.85 (d, $J = 8.7$ Hz, 1H; 5′-H), 6.85 (s, 1H; –CH=), 4.01 (s, 3H; OMe), 2.37 ppm (s, 3H; OAc); ^{13}C NMR (100 MHz, $CDCl_3$): $\delta = 182.9$ (C-3), 168.4 (C-6), 166.5 (C-8), 164.7 (OCOMe), 157.3 (C-4′), 150.9 (C-2′), 147.0 (C-2), 140.3 (C-6′), 125.6 (C-4), 121.9 (C-1′), 119.3 (C-9), 117.6 (C-5), 111.6 (–CH=), 110.1 (C-5′), 106.7 (C-7), 53.8 (OMe), 21.2 ppm (OCOMe); MS (ESI): *m/z*: 312 $[M+H]^+$, 334 $[M+Na]^+$; elemental analysis calcd (%) for $C_{17}H_{13}NO_5 \cdot {}^1/_4 H_2O$: C 64.66, H 4.28, N 4.44; found: C 64.18, H 4.02, N 4.49.

(*Z*)-6-Acetoxy-2-((6-methoxy-1-oxypyridin-3-yl)methylene)benzofuran-3(2*H*)-one (5): Urea hydrogen peroxide adduct (1.28 g, 12.88 mmol) was added at 0 °C to a solution of (*Z*)-6-acetoxy-2-((6-methoxypyridin-3-yl)methylene)benzofuran-3(2*H*)-one **4** (1 g, 3.22 mmol) in dichloromethane (40 mL), followed by the addition of trifluoroacetic anhydride (1.79 mL, 12.88 mmol). The mixture was stirred at room temperature for 16 h and was then diluted with dichloromethane, washed successively with sodium thiosulfate, water, and brine, dried over magnesium sulfate, and concentrated under reduced pressure. The residue was purified by silica gel column chromatography (dichloromethane/methanol, 98:2 then 90:10 gradient elution) to afford the title compound (658 mg, 63%) as a yellow solid: m.p. 155–157 °C; ^{1}H NMR (400 MHz, $CDCl_3$): $\delta = 8.95$ (d, $J = 2.0$ Hz, 1H; 2′-H), 7.77 (d, $J = 8.3$ Hz, 1H; 4-H), 7.65 (dd, $J_1 = 8.7$ Hz, $J_2 = 2.0$ Hz, 1H; 6′-H), 7.13 (d, $J = 1.8$ Hz, 1H; 7-H), 6.97 (dd, $J_1 = 8.3$ Hz, $J_2 = 1.8$ Hz, 1H; 5-H), 6.96 (d, $J = 8.7$ Hz, 1H; 5′-H), 6.60 (s, 1H; –CH=), 4.13 (s, 3H; OMe), 2.35 ppm (s, 3H; OAc); ^{13}C NMR (100 MHz, $CDCl_3$): $\delta = 182.8$ (C-3), 168.4 (C-6), 166.8 (C-8), 158.9, 157.9 (C-4′, OCOMe), 148.0 (C-2), 141.5 (C-2′), 130.4 (C-6′), 125.9 (C-4), 123.5 (C-1′), 118.8 (C-9), 118.4 (C-5), 107.7 (C-5′), 107.0 (C-7), 106.6 (–CH=), 57.7 (OMe), 21.4 ppm (OCOMe); MS (ESI): *m/z*: 328 $[M+H]^+$, 350 $[M+Na]^+$; elemental analysis calcd (%) for $C_{17}H_{13}NO_6 \cdot {}^1/_2 H_2O$: C 60.71, H 4.16, N 4.16; found: C 60.74, H 4.08, N 4.41.

(*Z*)-6-Hydroxy-2-((6-hydroxy-1-oxypyridin-3-yl)methylene)benzofuran-3(2*H*)-one (2): An aqueous solution of hydrochloric acid (10%, 4 mL) was added to a solution of (*Z*)-6-acetoxy-2-((6-methoxy-1-oxypyridin-3-yl)methylene)benzofuran-3(2*H*)-one (**5**, 400 mg, 1.22 mmol) in methanol (6 mL) and the mixture was heated at reflux for 16 h. After cooling, the precipitate was filtered and washed successively with water, methanol, and diethyl ether to afford the title compound (274 mg, 83%) as a white solid: m.p. >280 °C; ^{1}H NMR (400 MHz, DMSO): $\delta = 12.19$ (br s, 1H; OH), 11.17 (s, 1H; OH), 8.56 (s, 1H; 2′-H), 8.08 (d, $J = 9.2$ Hz, 1H; 6′-H), 7.59 (d, $J = 8.2$ Hz, 1H; 4-H), 6.78 (s, 1H; 7-H), 6.72 (s, 1H; –CH=), 6.65–6.70 ppm (m, 2H; 5,5′-H); ^{13}C NMR (100 MHz, DMSO): $\delta = 180.7$ (C-3), 167.3 (C-6), 166.3 (C-8), 157.0 (C-4′), 146.1 (C-2), 139.5 (C-2′), 138.6 (C-6′), 125.8 (C-4), 119.4 (C-1′), 113.0 (C-7,9), 110.6 (C-5′), 107.2 (–CH=), 98.6 ppm (C-5); MS (ESI): *m/z*: 270 $[M-H]^-$; elemental analysis calcd (%) for $C_{14}H_9NO_5 \cdot {}^1/_4 H_2O$: C 60.98, H 3.45, N 5.08; found: C 60.73, H 3.19, N 5.22.

Enzymatic assays: Mushroom tyrosinase (6.4 mg, purchased from Sigma) was dissolved in phosphate buffer (pH 7.0, 50 mM, 5 mL) and purified on Q-Sepharose FF with use of a gradient of NaCl from 0 to 1.0 M.[13] Purity of the tyrosinase was checked by SDS-PAGE; the purified tyrosinase exhibits only two bands at $M_W \approx 14$ kDa and 45 kDa. The tyrosinase activity was checked spectroscopically with use of L-DOPA as substrate (Figure S1).

All compounds were dissolved in DMSO stock solution (10%). Phosphate buffer (pH 7.0) was used to dilute the DMSO stock solu-

tions of the compounds. Mushroom tyrosinase (6 units, 6.4 μg mL^{-1}) was first pre-incubated with the compounds in phosphate buffer (pH 7.0, 50 mM) at 25 °C for 5 min. The L-DOPA (2 mM) was then added to the reaction mixture and the enzyme reaction was monitored by measuring the change in absorbance at 475 nm ($\varepsilon = 3600\ M^{-1}\ cm^{-1}$) of the DOPAchrome for 5 min.

DFT calculations: Theoretical calculations were based on density functional theory (DFT) and performed with the Gaussian 03 package.[22] Full geometry optimizations were carried out for all systems with use of the hybrid functional B3LYP[23] and the 6–31g* basis set on all atoms.[24] Vibrational frequency calculations were performed to ensure that each geometry optimization converged to a real minimum. Energetic analysis was carried out from additional single-point high-spin and broken-symmetry[25] calculations on the previously optimized geometries. For that purpose, the B3LYP functional was used together with a general basis set (6–311G* for Cu and coordinating O atoms,[26] 6–31G* for all remaining atoms). For the broken-symmetry state, the single-point calculation was performed with use of the high-spin wave function and the guess = (read, mix) keyword to generate the unrestricted broken-symmetry singlet wave function. The counterpoise (CP) procedure was used to correct the total energy for the basis set superposition error (BSSE).[27] Magnetic properties were evaluated from the same high-spin and broken-symmetry calculations as employed for energetic analysis. The Yamaguchi formula[28] was used to estimate the isotropic exchange coupling constants *J*.

Acknowledgements

The authors thank the French Agence Nationale pour la Recherche for financial support (ANR-09-BLAN-0028-01/02/03) and for grants to M.O., C.B., and C.D. The authors are grateful to the European COST Program in the framework of which this work was carried out (COST action CM1003 WG 2).

Keywords: aurone · DFT calculations · enzyme activators · enzyme inhibitors · mushroom tyrosinase

[1] E. I. Solomon, U. M. Sundaram, T. E. Machonkin, *Chem. Rev.* **1996**, *96*, 2563 – 2605.
[2] M. Rolff, J. Schottenheim, H. Decker, F. Tuczek, *Chem. Soc. Rev.* **2011**, *40*, 4077 – 4098.
[3] V. N. Sehgal, G. Srivastava, *Int. J. Dermatol.* **2008**, *47*, 1041 – 1050; R. E. Boissy, J. J. Nordlund, *Pigment Cell Res.* **1997**, *10*, 12 – 24.
[4] Y. Xu, A. H. Stockes, W. M. Freeman, S. C. Kumer, B. A. Vogt, K. E. Vrana, *Mol. Brain Res.* **1997**, *45*, 159 – 162.
[5] C. Visús, R. Andres, J. I. Mayordomo, M. J. Martinez-Lorenzo, L. Murillo, B. Sáez-Gutiérrez, C. Diestre, I. Marcos, P. Astier, J. Godino, F. J. Carapeto-Marquez de Prado, L. Larrad, A. Tres, *Melanoma Res.* **2007**, *17*, 83 – 89.
[6] S.-Y. Seo, V. K. Sharma, N. Sharma, *J. Agric. Food Chem.* **2003**, *51*, 2837 – 2853; Y.-J. Kim, H. Uyama, *Cell. Mol. Life Sci.* **2005**, *62*, 1707 – 1723; T.-S. Chang, *Int. J. Mol. Sci.* **2009**, *10*, 2440 – 2475.
[7] S. Okombi, D. Rival, S. Bonnet, A. M. Mariotte, E. Perrier, A. Boumendjel, *J. Med. Chem.* **2006**, *49*, 329 – 333.
[8] S. Takahashi, T. Kamiya, K. Saeki, T. Nezu, S.-I. Takeuchi, R. Takasawa, S. Sunaga, A. Yoshimori, S. Ebizuka, T. Abe, S.-I. Tanuma, *Bioorg. Med. Chem.* **2010**, *18*, 8112 – 8118.
[9] J. S. Chen, C. Wei, M. R. Marshall, *J. Agric. Food Chem.* **1991**, *39*, 1897 – 1901; R. C. Hider, K. Lerch, *Biochem. J.* **1989**, *257*, 289 – 290.
[10] M. T. Hassan Khan, M. I. Choudhary, A. U. Rahman, R. P. Mamedova, M. A. Agzamova, M. N. Sultankhodzhaev, M. I. Isaev, *Bioorg. Med. Chem.* **2006**, *14*, 6085 – 6088.
[11] E. Peyroux, W. Ghattas, R. Hardré, M. Giorgi, B. Faure, A. J. Simaan, C. Belle, M. Réglier, *Inorg. Chem.* **2009**, *48*, 10874 – 10876.
[12] J. L. Major Jourden, S. M. Cohen, *Angew. Chem.* **2010**, *122*, 6947 – 6949; *Angew. Chem. Int. Ed.* **2010**, *49*, 6795 – 6797; J. L. Major Jourden, S. M. Cohen, *Chem. Commun.* **2010**, *46*, 1241 – 1243; M. A. Chowdhury, H. Chen, K. R. A. Abdellatif, Y. Dong, K. C. Petruk, E. E. Knaus, *Bioorg. Med. Chem. Lett.* **2008**, *18*, 4195 – 4198; F. E. Jacobsen, R. M. Breece, W. K. Myers, D. L. Tierney, S. M. Cohen, *Inorg. Chem.* **2006**, *45*, 7306 – 7315; J. A. Lewis, J. Mongan, J. A. McCammon, S. M. Cohen, *ChemMedChem* **2006**, *1*, 694 – 697; D. T. Puerta, M. O. Griffin, J. A. Lewis, D. Romero-Perez, R. Garcia, F. J. Villarreal, S. M. Cohen, *J. Biol. Inorg. Chem.* **2006**, *11*, 131 – 138; D. T. Puerta, J. Lewis, S. M. Cohen, *J. Am. Chem. Soc.* **2004**, *126*, 8388 – 8389; D. T. Puerta, S. M. Cohen, *Inorg. Chem.* **2003**, *42*, 3423 – 3430.
[13] S. Yamazaki, S. Itoh, *J. Am. Chem. Soc.* **2003**, *125*, 13034 – 13035.
[14] A. Cornish-Bowden, *Fundamentals of Enzyme Kinetics*, Portland, London, **1995**.
[15] J. C. Espín, H. J. Wichers, *J. Agric. Food Chem.* **1999**, *47*, 3518 – 3525.
[16] J. C. Espín, H. J. Wichers, *J. Agric. Food Chem.* **1999**, *47*, 3503 – 3508.
[17] A. Rescigno, E. Sanjust, G. Soddu, A. C. Rinaldi, F. Sollai, N. Curreli, A. Rinaldi, *Biochim. Biophys. Acta* **1998**, *1384*, 268 – 276.
[18] E. Sanjust, G. Cecchini, F. Sollai, N. Curreli, A. Rescigno, *Arch. Biochem. Biophys.* **2003**, *412*, 272 – 278.
[19] W. T. Ismaya, H. J. Rozeboom, A. Weijn, J. J. Mes, F. Fusetti, H. J. Wichers, B. Dijkstra, *Biochemistry* **2011**, *50*, 5477 – 5486.
[20] C. Beney, A.-M. Mariotte, A. Boumendjel, *Heterocycles* **2001**, *55*, 967 – 972.
[21] S. Torelli, C. Belle, I. Gautier Luneau, J. L. Pierre, E. Saint Aman, J. M. Latour, L. Le Pape, D. Luneau, *Inorg. Chem.* **2000**, *39*, 3526 – 3536.
[22] Gaussian 03 (Revision A1), M. J. Frisch, G. W. Trucks, H. B. Schlegel, G. E. Scuseria, M. A. Robb, J. R. Cheeseman, V. G. Zakrzewski, J. A. Montgomery, J. R. E. Stratmann, J. C. Burant, S. Dapprich, J. M. Millam, A. D. Daniels, K. N. Kudin, M. C. Strain, O. Farkas, J. Tomasi, V. Barone, M. Cossi, R. Cammi, B. Mennucci, C. Pomelli, C. Adamo, S. Clifford, J. Ochterski, G. Petersson, A. P. Y. Ayala, Q. Cui, K. Morokuma, D. K. Malick, A. D. Rabuck, K. Raghavachari, J. B. Foresman, J. Cioslowski, J. V. Ortiz, A. G. Baboul, B. B. Stefanov, G. Liu, A. Liashenko, P. Piskorz, I. Komaromi, R. Gomperts, R. L. Martin, D. J. Fox, T. Keith, M. A. Al-Laham, C. Y. Peng, A. Nanayakkara, M. Challacombe, P. M. W. Gill, B. Johnson, W. Chen, M. W. Wong, J. L. Andres, C. Gonzalez, M. Head-Gordon, J. A. Pople, revision A.1. ed. Gaussian, Inc., Pittsburg PA., **2003**.
[23] A. D. Becke, *J. Chem. Phys.* **1993**, *98*, 5648 – 5652; C. Lee, W. Yang, R. G. Parr, *Phys Rev. B* **1988**, *37*, 785 – 789.
[24] P. C. Hariharan, J. A. Pople, *Theor. Chim. Acta* **1973**, *28*, 213 – 222; P. C. Hariharan, J. A. Pople, *Mol. Phys.* **1974**, *27*, 209 – 214.
[25] L. Noodleman, *J. Chem. Phys.* **1981**, *74*, 5737 – 5743; L. Noodleman, D. A. Case, *Adv. Inorg. Chem.* **1992**, *38*, 423 – 470; L. Noodleman, E. R. Davidson, *Chem. Phys.* **1986**, *109*, 131 – 143.
[26] R. Krishnan, J. S. Binkley, R. Seeger, J. A. Pople, *J. Chem. Phys.* **1980**, *72*, 650 – 654.
[27] S. F. Boys, F. Bernardi, *Mol. Phys.* **1970**, *19*, 553 – 566; S. Simon, M. Duran, J. J. Dannenberg, *J. Chem. Phys.* **1996**, *105*, 11024 – 11031.
[28] T. Soda, Y. Kitagawa, T. Onishi, Y. Takano, Y. Shigeta, H. Nagao, Y. Yoshika, K. Yamaguchi, *Chem. Phys. Lett.* **2000**, *319*, 223 – 230; K. Yamaguchi, Y. Takahara, T. Fueno in *Applied Quantum Chemistry* (Ed.: V. H. Smith), Reidel, Dordrecht, **1986**.

Received: November 14, 2011
Published online on February 3, 2012

